

# Electrochemical oxidation of dibenzothiophene compounds on BDD electrode in acetonitrile–water medium

O. Ornelas Dávila<sup>a</sup>, L. Lacalle Bergeron<sup>b</sup>, P. Ruiz Gutiérrez<sup>c</sup>, M. M. Dávila Jiménez<sup>a,\*</sup>, I. Sirés<sup>d</sup>, E. Brillas<sup>d</sup>, A.F. Roig Navarro<sup>b</sup>, J. Beltrán Arandes<sup>b</sup>, J.V. Sancho Llopis<sup>b</sup>

<sup>a</sup> *Facultad de Ciencias Químicas, Benemérita Universidad Autónoma de Puebla, Mexico*

<sup>b</sup> *Instituto Universitario de Plaguicidas y Aguas (IUPA), Universidad Jaume I, Castellón de la Plana, Spain*

<sup>c</sup> *Centro de Química Instituto de Ciencias, Benemérita Universidad Autónoma de Puebla, Mexico*

<sup>d</sup> *Laboratori d'Electroquímica dels Materials i del Medi Ambient, Departament de Química Física, Facultat de Química, Universitat de Barcelona, Martí i Franquès 1-11, 08028 Barcelona, Spain*

\* Corresponding author: E-mail address: mdavila.uap.mx@gmail.com

Tel.: +52-222-229-5525

**Abstract**

The electrochemical oxidation of dibenzothiophene and two derivatives, namely 4-methyldibenzothiophene and 4,6-dimethyldibenzothiophene, was investigated either separately or as a mixture, on a BDD anode in a miscible acetonitrile (87.5% v/v)–water (12.5% v/v, 0.01 M NaNO<sub>3</sub>) solution. Linear sweep voltammetry, cyclic voltammetry, chronoamperometry and bulk electrolysis under potentiostatic conditions suggested the probable occurrence of two pathways: direct electrochemical oxidation and indirect reaction with hydroxyl radicals and other reactive oxygen species formed at the BDD anode surface during water discharge. The products extracted upon electrolysis at 1.5 and 2.0 V vs. SCE were analyzed by Fourier-transform infrared spectroscopy, gas chromatography–mass spectrometry and ultra-high performance liquid chromatography coupled to electrospray ionization and quadrupole time-of-flight mass spectrometry (UHPLC-ESI-Q-TOF-MS). The main molecules identified were the corresponding sulfoxides or sulfones, depending on the applied anodic potential. Possible oxidation routes for the dibenzothiophene compounds are proposed.

*Keywords:* BDD; Dibenzothiophenes; Electrochemical desulfurization; Sulfone; Sulfoxide

## 1. Introduction

The oxidation of alkyl sulfides is of considerable interest for practical applications, particularly in the hydrodesulfurization (HDS) of liquid fuels. Current HDS technologies are effective when applied to aliphatic and cyclic sulfur compounds but are less effective for the treatment of aromatic ones. These latter include dibenzothiophene (DBT) and derivatives such as 4-methyldibenzothiophene (4-MDBT) and 4,6-dimethyldibenzothiophene (4,6-DMDBT) (see molecular structures in Fig. 1), along with other derivatives present in diesel [1,2]. In recent years, oxidative desulfurization (ODS) has been recognized as a promising alternative process for sulfur removal [3-6], thus complementing current HDS technologies. Through the ODS process, refractory dibenzothiophene compounds and their alkylated derivatives present in liquid fuels can be converted into very polar sulfoxides or sulfones under mild conditions. Further, these products can be selectively extracted with various solvents [7,8].

A variety of oxidants may be used in the ODS process. Among these,  $\text{H}_2\text{O}_2$  is attractive because it is commercially available and relatively cheap. This species can be combined in multiple ways:  $\text{H}_2\text{O}_2$ /acetic acid [9],  $\text{H}_2\text{O}_2$ /formic acid [10], and  $\text{H}_2\text{O}_2$ /heterogeneous catalyst [10,11]. Other reactive oxygen species (ROS) such as  $\text{O}_3$ ,  $\text{O}_2^{\bullet-}$  and  $\bullet\text{OH}$  can also oxidize the organic substances. These highly reactive species can be generated *in situ* by electrolysis of water present in the medium or upon the electrolyte decomposition [12–14]. In this context, electrochemical oxidation has been proposed as an effective alternative for removing sulfur, especially from diesel and gasoline.

Several articles have focused on electrochemical desulfurization (ECDS) as a new approach to liquid fuel desulfurization [15-20]. The ECDS method is advantageous compared to HDS since it is carried out at low reaction temperatures and pressures, in the absence of hydrogen. During the electrochemical oxidation under optimized working

conditions, sulfur aromatic compounds and their derivatives are easily oxidized to the corresponding sulfoxides and sulfones by direct electron transfer. These oxidized products can be subsequently removed by liquid-liquid extraction or adsorption techniques [21-24]. Simultaneously, ROS can also be produced from water electro-oxidation using anodes having different compositions, morphologies and structural properties [25-28]. ROS are then localized at an interface (e.g., electrode–solution, catalyst–solution). The most commonly employed electrodes to generate oxidizing species include vitreous carbon,  $\text{PbO}_2$ , dimensionally stable anodes (DSA<sup>®</sup>) and boron-doped diamond (BDD) [29]. The BDD electrode is the most efficient anode to mineralize contaminants like pesticides, dyes or drugs [30,31] contained in wastewater, which is due to its high oxidation power and large oxygen evolution overpotential. In some cases, however, it is not necessary to achieve total mineralization, but only to convert the parent molecule into more polar compounds that can be subsequently extracted from the medium. Oxidation studies on aromatic sulfur compounds have been carried out either in aprotic or aqueous media. However, less is known when mixtures of an aprotic medium and water are employed and, more important, which is the contribution of water in the reaction route. To gain deeper knowledge on the role of water in the ODS of dibenzothiophenes when mixed with acetonitrile, an exhaustive study dealing with the electrochemical reactivity of DBT, 4-MDBT and 4,6-DMDBT has been undertaken for the first time. This has allowed clarifying the reaction mechanisms to yield their respective sulfoxides or sulfones under mild electrolysis conditions using a BDD anode. Electroanalytical techniques like linear sweep voltammetry, cyclic voltammetry, chronoamperometry and bulk electrolysis, as well as analytical methods like FTIR, UV/Vis, UHPLC-ESI-Q-TOF-MS and GC-MS, have been utilized. The contributions of direct and mediated oxidation during the electro-oxidation process of benzothiophenes were examined and reliable oxidation pathways for each compound were elucidated.

## 2. Materials and methods

### 2.1. Reagents and preparation of solutions

DBT (99% purity), 4-MDBT (96% purity), 4,6-DMDBT (97% purity), methanol and hexane of chromatographic grade, and  $\text{NaNO}_3$  were purchased from Sigma Aldrich. Acetonitrile ACS/HPLC provided by Burdick & Jackson and ultrapure water ( $18.2 \text{ M}\Omega \cdot \text{cm}$ ) from a Milli-Q system were used to prepare the acetonitrile/water solutions. For the electrochemical studies, single solutions were prepared by dissolving DBT, 4-MDBT or 4,6-DMDBT, separately, first in acetonitrile for 30–45 min with mechanical stirring. Then, the appropriate volumes of 0.01 M  $\text{NaNO}_3$  aqueous solution were added to obtain an acetonitrile (87.5% v/v)–water (12.5% v/v, 0.01 M  $\text{NaNO}_3$ ) mixture. DBT + 4-MDBT + 4,6-DMDBT mixtures in the above medium were also prepared to clarify the electrochemical reactivities.

### 2.2. Electrochemical analysis

DBT and its alkylated derivatives 4-MDBT and 4,6-DMDBT are poorly soluble in water and confer low conductivity. Therefore, acetonitrile was employed as a co-solvent and  $\text{NaNO}_3$  as the electrolyte. The acetonitrile (87.5% v/v)–water (12.5% v/v, 0.01 M  $\text{NaNO}_3$ ) mixture was suitable for investigating the electrochemical oxidation and bulk electrolysis of all dibenzothiophenes. First, the BDD electrode was cycled (over 5 cycles) from  $-2.00$  to  $2.00 \text{ V}$  vs. SCE at  $10 \text{ mV s}^{-1}$  in a given solution. The electrochemical measurements and bulk electrolyses of the dibenzothiophenic compounds were carried out in an undivided cell of 80 mL comprising three electrodes and the acetonitrile (87.5% v/v)–water (12.5% v/v, 0.01 M  $\text{NaNO}_3$ ) medium. The anode and counter electrode were commercial boron-doped diamond (BDD) thin films deposited onto niobium mesh substrates, purchased from Condias (Germany), with a geometrical area of  $20 \text{ cm}^2$  each. SCE (3 M KCl) was employed as the

reference electrode, and all potentials are referred to it. The electrochemical measurements were carried out using an Autolab PGSTAT 302 potentiostat/galvanostat from Eco Chemie, controlled by GPES 4.9 software. The electrochemical response and stability of the BDD anode was tested by recording cyclic voltammograms before and after each experiment.

### 2.3. Equipment and analysis conditions

#### 2.3.1. GC-MS analysis

After evaporating the electrolyzed solutions, the solid phase was dissolved in methanol and hexane to analyze the oxidized products using gas chromatography (GC) equipped with an ion-trap mass spectrometer (MS). A Varian CP-3800 gas chromatograph coupled to a mass spectrometry detector (Saturn 4000, Varian) was used to identify the molecules, which were separated on a Supelcowax 10 (30 m × 0.25 mm, 0.25 μm film thickness) capillary column, using helium as carrier gas at a constant flowrate of 1 mL min<sup>-1</sup>. The temperature program was: 70 °C for 2 min, increase to 150 °C at 30 °C min<sup>-1</sup> and then, increase to 250 °C at 5 °C min<sup>-1</sup>, with a final isothermal stage of 25.33 min. Injection of 1 μL of sample in splitless mode (injection port temperature of 220 °C) was performed using a Varian 8400 autosampler equipped with a 10 μL syringe. Ion trap MS determinations were carried out in full scan mode (*m/z* scan range of 40 – 600 Da) using electron impact ionization (70 eV) in positive mode and external ionization configuration. GC-MS interface; ion trap and manifold temperatures were set at 275 °C, 190 °C and 60 °C, respectively.

#### 2.3.2. UHPLC-ESI-Q-TOF-MS analysis

The electrolyzed solutions were concentrated by evaporation. Then, they were diluted (1:100) for the analysis of the products by UHPLC-ESI-Q-TOF-MS. The modern Q-TOF-MS instruments allow the simultaneous acquisition of two full spectra acquisition functions with different collision energies in a single injection (MSE mode). Using the low

energy function (LE) with a collision energy of 4 eV, the information obtained corresponds normally to non-fragmented ions, related to the parent protonated molecule  $[M+H]^+$  in positive ionization mode. The high energy function (HE), with a collision energy ramp ranging from 15 to 40 eV, is selected in order to obtain a wide range of fragmented ions.

The analysis was carried out with a Waters Acquity ultra-performance liquid chromatography (UPLC) system (Waters, Milford). The chromatographic separation was performed using an Acquity UPLC BEH C18 (2.1 mm  $\times$  100 mm, 1.7  $\mu$ m particle size) analytical column from Waters. The mobile phases used were A (water) and B (methanol), both with 0.01% formic acid. The percentage of B changed as follows: 0 min, 10%; 14 min, 90%; and 16.10 min, 10%. The flowrate was 300  $\mu$ L  $\cdot$  min<sup>-1</sup> and the analysis run time was 18 min. The sample injection volume was 20  $\mu$ L. The UPLC system was interfaced to a hybrid quadrupole-TOF high resolution (HRMS) mass spectrometer (Xevo G2 Q-TOF, Waters Micromass), using an orthogonal Z-spray-ESI interface operating in both positive and negative ion mode. TOF-MS resolution was approximately 25000 at full width half maximum at  $m/z$  556. Nitrogen was used as drying gas and nebulizing gas. The gas flow was set at 800 L  $\cdot$  h<sup>-1</sup>. MS data were acquired over an  $m/z$  range of 50-1200 at a scan time of 0.4 s. A capillary voltage of 0.7 kV and cone voltage of 20 V were used in positive ionization mode. Collision gas was argon 99.995% (Praxair). The interface, source and column temperatures were set at 450  $^{\circ}$ C, 150  $^{\circ}$ C, and 40  $^{\circ}$ C, respectively.

### 2.3.3. ICP-MS analysis

Qualitative determination of niobium in electrolyzed solutions was conducted with an Agilent 7500cx ICP-MS instrument. For that purpose, the selected samples were evaporated to dryness and redissolved with 2 mL of 1% HNO<sub>3</sub>. Afterwards, samples were nebulized to the ICP-MS and  $m/z$  93 was monitored in qualitative mode (20 points per peak). Reagents free of Nb were checked from the analysis of blank solutions (1% HNO<sub>3</sub>).

#### 2.3.4. UV/Vis analysis and FTIR spectroscopy

Hydrogen peroxide formed during the electrolysis in the reaction medium was analyzed using UV/Vis spectrophotometry (HACH DR 5000) over the range 200–800 nm. The IR spectra were recorded over the range 400–4000  $\text{cm}^{-1}$  using a Nicolet 6700 spectrometer from Thermo Scientific and pressed KBr pellets.

### 3. Results and discussion

#### 3.1. Electrochemical response of the BDD electrode in acetonitrile–water medium

Linear sweep and cyclic voltammograms were recorded in water and in acetonitrile–water mixtures containing 0.01 M  $\text{NaNO}_3$  as the electrolyte. Different acetonitrile and water proportions were used and DBT was added to test the electrochemical response of the BDD working electrode and the discharge of water and solvent. The linear sweep voltammograms obtained in the different electrolytic media are shown in Fig. 2. These curves were recorded from -0.50 V, although they are presented starting from 0.50 V to better observe the oxidation process. The use of 12.5% water with 0.01 M  $\text{NaNO}_3$  yielded a greater anodic current due to the decomposition of water present in the reaction medium (Fig. 2, curve (a)). The anodic current increased considerably in the presence of a much larger amount of water, i.e., 87.5% (Fig. 2, curve (b)). In acetonitrile (12.5%)–water (87.5%, 0.01 M  $\text{NaNO}_3$ ) or in 100% water with 0.01 M  $\text{NaNO}_3$  (Fig. 2, curve (c)), the onset potential for water discharge was less anodic (see inset of Fig. 2). In these cases, the anodic current was high in the potential range 1.50–2.00 V (Fig. 2, curves (b) and (c)). The onset potentials were of 1.655, 1.386 and 1.524 V in acetonitrile (87.5%)–water (12.5%), acetonitrile (12.5%)–water (87.5%) and 100% water, respectively.



On the other hand, oxygen evolution from water oxidation on a BDD electrode requires a large overpotential and the mechanism involves the formation of  $\bullet\text{OH}$  as intermediate in the oxygen evolution reaction. According to some authors [13,32], a decrease in the oxygen evolution rate occurs in the presence of aprotic and protic solvents due to competition with  $\bullet\text{OH}$ . The latter may be responsible for the low current observed within the potential interval from 1.50 to 2.00 V in the presence of an excess of acetonitrile.

### 3.2. Linear polarization curves for the electrochemical oxidation of DBT, 4-MDBT and 4,6-DMDBT

The electrochemical behavior of DBT, 4-MDBT, and 4,6-DMDBT on BDD was studied separately by means of linear sweep voltammetry. Fig. 3a shows the profiles obtained in the absence of dibenzothiophenes as well as in the presence of  $67\text{ mg L}^{-1}$  DBT (curve (a)),  $86\text{ mg L}^{-1}$  4-MDBT (curve (b)) and  $86\text{ mg L}^{-1}$  4,6-DMDBT (curve (c)). These concentrations were selected so as to ensure the good resolution of peaks. These curves revealed no obvious oxidation peaks, although subtraction of the background electrolyte current in Fig. 3b shows a maximum current near the onset decomposition potential of water for DBT (curve (a')), 4-MDBT (curve (b')) and 4,6-DMDBT (curve (c')). The potentials at which the maximum anodic currents appeared were 1.96, 1.90 and 1.91 V for such compounds, respectively. This means that the three dibenzothiophenes are directly oxidized at the BDD surface before water discharge, although their removal is enhanced when the latter process occurs since it yields the strong oxidant  $\bullet\text{OH}$ , which promotes the mediated oxidation. These peaks can be attributed to the formation of sulfone groups ( $\text{DBTO}_2$ ) via oxidation of the corresponding dibenzothiophene sulfoxide (DBTO), as demonstrated below. Note that the formation of  $\text{DBTO}_2$  around 2.00 V on a glassy carbon electrode in acetonitrile medium and in the presence of water has been previously reported [33].

The above linear voltammograms also revealed that, at potential values exceeding the onset value of 1.165 V, the anodic currents increased markedly. This trend was attributed to the direct electro-oxidation of the dibenzothiophene compounds and, at potentials higher than 1.9 V, to the decomposition of water present in the reaction medium, which generated reactive oxidants such as  $\cdot\text{OH}$ ,  $\text{O}_3$ ,  $\text{H}_2\text{O}_2$  and  $\text{O}_2$  [25,29]. On the other hand, the onset oxidation potentials for 67 mg L<sup>-1</sup> DBT and 86 mg L<sup>-1</sup> 4-MDBT were very similar and slightly higher than 1.224 V (curves (a') and (b') in Fig. 3b). The 86 mg L<sup>-1</sup> 4,6-DMDBT profile revealed a much lower onset oxidation potential of 0.790 V (curve (c')). In addition, a small oxidation peak appeared around 1.038 V (Fig. 3a and b, curves (c) and (c')) within the region of the water stability (Fig. 2). The anodic peak that appeared at 1.038–1.150 V within the low potential region, as well as the low maximum anodic current observed in Fig. 3b, curve (c'), suggests the electrochemical oxidation of 4,6-DMDBT by an electrochemical–chemical oxidation mechanism similar those proposed for DBT [33,34], diaryl sulfides [35] and aliphatic sulfides [36]. It means that the direct electrochemical oxidation of 4,6-DMDBT occurred in the potential region corresponding to water stability. This was corroborated upon bulk electrolysis of 4,6-DMDBT (86 mg L<sup>-1</sup>) at 1.15 V over a long period of time of 16 h. The main product identified in the electrolyzed extract by UHPLC-ESI-Q-TOF-MS was 4,6-dimethyldibenzothiophene sulfoxide (4,6-DMDBTO).

We aimed to study the electrochemical reactivity of DBT and 4,6-DMDBT by comparing the linear sweep voltammograms at a lower concentration of 20 mg L<sup>-1</sup> DBT and 4,6-DMDBT at 20 mV s<sup>-1</sup>, after subtracting the background electrolyte current (data not shown). These results showed that the first oxidation step occurred at 1649 mV for DBT and at 1580 mV for 4,6-DMDBT. On the other hand, the smaller anodic peak at 1.038–1.150 V suggested that 4,6-DMDBT was more electrochemically reactive than DBT. The reactivity of alkyl dibenzothiophenes in desulfurization processes could be described using theoretical

descriptors like the local, global and molecular electrostatic potential [37]. The oxidation reactivity of sulfur compounds is reported to increase with the electron density on the sulfur atom [7]. In this context, the higher electron densities (5.760) of the sulfur atoms in 4,6-DMDBT and 4-MDBT (5.759) rendered more favorable the anodic oxidation as compared to DBT (5.758). These results agree with the reactivity of DBT and alkyl dibenzothiophenes reported during oxidative desulfurization of light gas oil [7] and fuel oils using the ODS methods [10,11].

### 3.3. Cyclic voltammetry with DBT, 4-MDBT and 4,6-DMDBT solutions

The cyclic voltammograms for the oxidation of 67 mg L<sup>-1</sup> DBT and 86 mg L<sup>-1</sup> 4-MDBT and 4,6-DMDBT revealed that their oxidation on BDD surface occurred around 1.20 V, showing the highest anodic currents between 1.50 and 2.00 V (Fig. 4a, curves (a)–(c)). Worth commenting, all voltammograms were initiated at -2.00 V, near the cathodic discharge of water to hydrogen and OH<sup>-</sup>, although the profiles presented in Fig. 4 start at -0.50 V to better observe the anodic oxidation. No reduction peaks were found during the cathodic scans down to -2.00 V, meaning that the oxidation process was irreversible, probably due to the fast reactions of cation radicals (after abstracting one electron from sulfur) with water molecules present in the reaction medium [33-36].

The effect of electrode fouling was tested by recording consecutive cyclic voltammograms during the anodic oxidation of 200 mg L<sup>-1</sup> DBT and 4,6-DMDBT at a scan rate of 10 mV s<sup>-1</sup>. The changes in current during the first five cycles overlapped for 200 mg L<sup>-1</sup> DBT (Fig. 4b, curve (a)) and 4,6-DMDBT (Fig. 4b, curve (b)). The current at anodic potential ( $E_{an}$ ) = 2.00 V decreased by 9% after 44 cycles for 200 mg L<sup>-1</sup> 4,6-DMDBT (Fig. 4b, curve (b)). This behavior and the fact that no specific peaks were found in the voltammograms, indicates that the oxidation products resulting from the parent compounds did not adsorb onto BDD. On the other hand, the cyclic voltammograms revealed that the

anodic current in the presence of the sulfur compounds increased at potentials greater than 1.50 V, indicating their oxidation. For this reason, the anodic oxidations of DBT and 4,6-DMDBT were investigated by electrolysis at constant potential. The extracts obtained after bulk electrolysis of these molecules for 4 h at 1.50 V in acetonitrile (87.5% v/v)–water (12.5% v/v, 0.01 M NaNO<sub>3</sub>) were analyzed by GC-MS and UHPLC-ESI-Q-TOF-MS, confirming that DBTO and 4,6-dimethyldibenzothiophene sulfoxide (4,6-DMDBO) were formed at this potential pre-eminently via direct electrochemical oxidation. Bulk electrolysis at 2.00 V for 4 h yielded dibenzothiophene sulfone (DBTO<sub>2</sub>) and 4,6-dimethyldibenzothiophene sulfone (4,6-DMDBTO<sub>2</sub>) as the main products.

The anodic current depended on the concentration of the dibenzothiophene compounds present in the reaction medium. The potentiodynamic curves shown in Fig. 5a and b revealed that 30 mg L<sup>-1</sup> DBT (curve (a)) or 4, 6-DMDBT (curve (a')) presented one oxidation wave around 1.74 and 1.61 V, respectively. This figure also depicts that the onset for DBT oxidation was shifted to lower positive values at higher concentrations of the compound. The shifts of the *I-E* curves toward lower potentials indicated that DBT and 4,6-DMDBT oxidation also occurred through hydroxyl radicals. However, the anodic current was low in the interval potentials from 1.00 to 1.35 V, but increased dramatically at  $E_{an} > 1.35$  V. This behavior of the oxidation current as a function of the potential and concentration evidences that DBT and 4,6-DMDBT oxidation processes were accompanied by other oxidation reactions that occurred simultaneously. Fig. 5a and b also indicate that the anodic current depended strongly on the sulfur compound concentration, reaching potentials exceeding 1.75 V, where water decomposition occurred. For this reason, at  $E_{an} > 1.75$  V, the indirect oxidation of sulfur compounds can be assumed, mediated by electrogenerated •OH (and other ROS), along with direct electron transfer at the BDD anode surface. The water oxidation then contributed to the total anodic current. The shift of the onset values for of DBT and

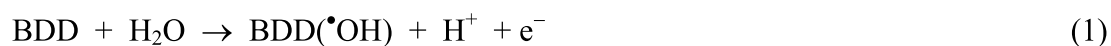
4,6-DMDBT oxidation and the dependence of the maximum anodic current on concentration were more evident when the background current was subtracted upon linear polarization (Fig. 6a and b). These curves revealed a linear dependence of the anodic current on the concentration of compounds over a potential range between 1.25 and 1.90 V (insets in Fig. 6a and b). A linear dependence was also obtained when plotting  $I_p$  vs.  $v^{1/2}$  during the voltammetric studies, as expected if the oxidation of both, DBT and 4,6-DMDBT, was controlled by mass transport.

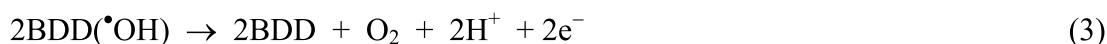
At high concentrations, the start of the anodic oxidation was more pronounced (insets showing  $E$  vs. concentration at a constant current). The low current in the potential region from 0.80 to 1.35 V for the dibenzothiophene compounds indicate that the direct oxidation process occurred and did not play a prominent role in the overall electrochemical oxidation. This is in agreement with the quasi-polarization curves of  $\log I$  vs.  $E$ , as shown in Fig. 5 (insets) for the electro-oxidation of DBT and 4,6-DMDBT at the BDD anode, where two Tafel slopes can be observed. The Tafel slopes for DBT in the low potential range varied from 262 to 271 mV dec<sup>-1</sup>, and the reaction order with respect to DBT was 0.62. In the case of 4,6-DMDBT, the Tafel slopes within the low potential range varied from 238 to 333 mV dec<sup>-1</sup> and the reaction order was 0.51. The high values of the Tafel slopes and the low reaction order possibly arose either from the BDD film deposit onto the porous Nb substrate [38,39] or from a first slow charge transfer step. These values also indicate that the oxidation of these compounds occurred through a multi-stage mechanism, as described previously [33-36]. The feasible mechanism (direct or indirect oxidation) operating at  $E_{an} < 1.50$  V or  $1.70 \leq E_{an} \leq 2.00$  V was explored using chronoamperometric measurements.

#### 3.4. Chronoamperometric study

In an anhydrous aprotic solvent, it is easy to discern whether the oxidation of an organic compound occurs via direct oxidation; however, the electrochemical oxidation of the

dibenzothiophenic compounds in acetonitrile–water was very difficult to characterize in terms of direct electron transfer or mediated oxidation mechanisms. Chronoamperometric experiments were carried out to study the electrochemical oxidation of DBT or 4,6-DMDBT within the potential interval 1.15–2.00 V. Fig. 7 presents the potentiostatic  $I-t$  curves obtained for different 4,6-DMDBT concentrations at several applied potentials using quiescent solutions. As shown in these curves, the anodic current depended on the concentration of 4,6-DMDBT. The current difference between the electrolyte solution prepared with or without 4,6-DMDBT supported the direct transfer of electrons at the anode surface. Higher current reaction steps (i.e., the space between the current in the presence and absence of 4,6-DMDBT) indicated better direct electrochemical oxidation of the compound at the electrode surface. A low applied potential (1.150 V) produced no appreciable changes in the anodic currents of the 4,6-DMDBT solution or the electrolyte (Fig. 7a). These results allowed inferring that direct oxidation was not efficient, but, if the potential rose from 1.50 to 2.00 V, the anodic current increased significantly. At  $E_{an} \geq 1.50$  V, significant differences were observed between the steady state currents of the solution containing 4,6-DMDBT (Fig. 7b and c) and the supporting electrolyte. This evidences that oxidation occurred more favorably through direct electron transfer in this potential region. On the other hand, the  $I$  vs. concentration plots obtained at the three different potentials displayed a good linear dependence over the range 30–200 mg L<sup>-1</sup> (insets in Fig. 7), confirming the electrochemical decomposition of water and simultaneous direct electrochemical oxidation of 4,6-DMDBT. As previously reported [12,25], an acidic aqueous medium promotes the formation of hydroxyl radical and H<sub>2</sub>O<sub>2</sub> at the BDD electrode as a result of water discharge according to the following reactions:





In our case, the hydroxyl radical formed through direct electro-oxidation of water at the electrode surface (reaction (1)) facilitated the formation of  $\text{H}_2\text{O}_2$  near the electrode surface via reaction (2). The production of hydroxyl radical on the anode BDD surface was assessed by chronoamperometry measuring the current upon the step-by-step injection of water into the solution under polarization of the BDD anode at 1.75 or 2.00 V. As can be seen in Fig. 8a, the water addition to the reaction medium in the absence of 4,6-DMDBT caused a current increase (inset in Fig.8a). This finding agrees with the formation of hydroxyl radical on the anode surface via direct electron transfer according to reaction (1). At the same potential, in the presence of 4,6-DMDBT (Fig. 8b), a steady-state current was enhanced when its concentration was increased, as show in inset in Fig. 8b. This indicates that, at this potential, direct electron transfer occurred during 4,6-DMDBT oxidation in parallel with water discharge. Direct electron transfer in parallel to the indirect reaction of hydroxyl radicals has been reported for several organic pollutants [40,41]. Nevertheless, at  $E_{\text{an}} > 1.75$  V, the electrogenerated hydroxyl radicals may self-react to form  $\text{H}_2\text{O}_2$  by reaction (2) or evolve to  $\text{O}_2$  gas via reaction (3) [25].

The production of  $\text{H}_2\text{O}_2$  during the main electrolysis reaction in acetonitrile (87.5%)–water (12.5%, 0.01 M  $\text{NaNO}_3$ ) at 2.00 V was demonstrated using a spectrophotometric method based on the well-known formation of the Ti(IV)- $\text{H}_2\text{O}_2$  complex, as exemplified in SM Fig. S1.

### 3.5. Electrolyses under potentiostatic conditions

Bulk electrolysis assays for DBT, 4-MDBT and 4,6-DMDBT were carried out either with single compounds or with a mixture, at 1.50 and 2.00 V, for 4 h. During these trials, the anodic current at 2.00 V was higher than that at 1.50 V due to water oxidation. No passivation

of the BDD anode, as a result of possible fouling by polymerization of the target organic sulfur compounds or their by-products, was observed, as also described in the voltammetric study of section 3.3. Electrolysis at 2.00 V caused direct electro-oxidation and, in parallel, indirect reaction. A potential of  $E_{\text{an}} < 1.75$  V induced sulfur compound oxidation, as described above, through direct multi-stage electron transfer [33-36]. To better understand these points, analysis of the extracted products after bulk electrolysis was carried out by FTIR, GC-MS and UPLC-MS.

### 3.5.1. IR spectroscopic analysis of the extracted products

SM Fig. S2a-c depict the IR spectra of extracts of the dibenzothiophene compounds before and after oxidation. The infrared spectra obtained after electrochemical oxidation at 1.50 or 2.00 V revealed absorption bands corresponding to S-O vibrations in the range 600–500  $\text{cm}^{-1}$ . The C-S stretching frequencies between 700 and 800  $\text{cm}^{-1}$  shifted after oxidation of 4-MDBT (Fig. S2a) and 4,6-DMDBT (Fig. S2b). The IR spectra of samples treated at 1.50 and 2.00 V were compared with the spectra obtained from DBT-sulfone (Fig. S2c). All standard DBT-sulfone vibrations were present in the extracts of the treated samples. The sulfoxide and sulfone compounds formed were confirmed using GC-MS and UHPLC-ESI-Q-TOF-MS.

### 3.5.2. GC-MS analysis

After oxidation of the dibenzothiophene compounds at 1.50 and 2.00 V, the extracts were analyzed by GC-MS. SM Fig. S3a and S3b display the chromatograms and MS spectra corresponding to electrolysis of 4,6-DMDBT, whereas SM Fig. S4a and S4b show those of DBT. The peaks observed in the chromatograms obtained at retention time ( $t_r$ ) = 37.94 min (Fig. S4b, (b)) and  $t_r$  = 35.10 min (Fig. S3b, (b)), along with the MS spectra obtained at  $m/z$  =



216 (Fig. S4b) and  $m/z = 244$  (Fig. S3b), corresponded to the molecular ion peaks of DBTO<sub>2</sub> and 4,6-DMDBTO<sub>2</sub>, respectively, according with NIST database (match 84%). Analysis of the chromatograms shown in Fig. S3a and S4a revealed that the formation of 4,6-DMDBTO<sub>2</sub> was favored at 2.00 V, with the removal of 99.2% 4,6-DMDBT after 4 h of electrolysis. The removal of 97.5% DBT at the same potential required a greater electrolysis time of 6 h. These results suggests that 4,6-DMDBT was more prone to undergo anodic oxidation.

Bulk electrolysis of a model mixture containing DBT + 4-MDBT + 4,6-DMDBT was conducted over 4 h at 1.50 and 2.00 V with the aim of assessing the reactivity of each compound and possible interference (or interaction) between the three compounds. SM Fig. S5a and S5b show chromatograms and mass spectra obtained from solutions extracted with methanol after bulk electrolysis of a solution of dibenzothiophene compounds. An inspection of the chromatograms reveals that the peak areas of DBT, 4-MDBT and 4,6-DMDBT decreased markedly after bulk electrolysis at 2.00 V compared to 1.50 V, and the formation of the P1, P2, and P3 products were more favored at 2.00 V (Fig. S5a-(c)). These chromatograms evidence that the dibenzothiophene compounds were not completely oxidized at 1.50 V (Fig. S5a-(b)) or at 2.00 V (Fig. S5a-(c)) after 4 h of electrolysis. Few compounds remained in the mixture after electrolysis, since 99.4% DBT, 97.7% 4-MDBT and 99.7% 4,6-DMDBT were removed from the mixture. The mass spectra (Fig. S5b) highlight that the reaction products arising from the dibenzothiophene compounds in the mixture after electrolysis were DBTO<sub>2</sub>, 4-MDBTO<sub>2</sub> and 4,6-DMDBTO<sub>2</sub>. They were identified by comparing the retention times of pure compounds with NIST database. As shown in the chromatogram (c) of Fig. S5a, the simultaneous electrochemical oxidation of a mixture at 2.00 V preferably oxidized 4,6-DMDBT to its corresponding 4,6-DMDBTO<sub>2</sub> ( $t_r = 35.07$  min), as inferred from the intensity and area of the peak. These findings indicate that the sulfur compounds contained in the mixture were pre-eminently oxidized in the order:

4,6-DMDBT  $\geq$  4-MDBT  $>$  DBT. This agrees with the oxidation results obtained from ODS studies using different catalyst/hydroxide peroxide systems [11,17]. The oxidation products described above were confirmed using UHPLC-ESI-Q-TOF-MS analysis.

### 3.5.3. UHPLC-ESI-Q-TOF-MS analysis

The results obtained through UHPLC-ESI-Q-TOF-MS analysis of the extracts of DBT, 4-MDBT and 4,6-DMDBT at different potentials revealed that the electrochemical oxidation process at the BDD electrode in acetonitrile (87.5%)–water (12.5%, 0.01 M NaNO<sub>3</sub>) was a selective oxidation reaction. The total ion chromatograms of the oxidation products of 4-MDBT and 4,6-DMDBT after bulk electrolysis of each single compound at 2.00 V displayed only one peak at  $t_r$  of 7.24 and 8.43 min, respectively. Their mass spectra at low and high energy confirmed that the most important anodic oxidation products corresponded to 4-MDBTO<sub>2</sub> and 4,6-DMDBTO<sub>2</sub>, respectively. No other peaks were observed, meaning that there is no intermediate formation or degradation of the molecules under the analysis conditions. In the case of the simultaneous electrochemical oxidation of a mixture DBT + 4-MDBT + 4,6-DMDBT at 1.50 V, 4,6-DMDBT was preferably oxidized to 4,6-DMDBT sulfoxide (SM Fig. S6a). It can be seen in the chromatogram of Fig. S6b that the oxidation of the mixture at 2.00 V yielded the corresponding sulfones of DBT and 4-MDBT in a minor proportion. These results indicate that the 4,6-DMDBT oxidation is favored at 1.50 and 2.00 V and that the effect of the anodic potential is evident in the conversion of the sulfur compounds to their corresponding sulfoxides or sulfones. The mass spectra at low collision energy (LE) and high collision energy (HE) of the corresponding sulfoxides and sulfones are shown in the SM Fig. S7-S9. The 4,6-DMDBT oxidation was favored at  $E_{an} > 1.50$  V and  $E_{an} = 2.00$  V when it was present either alone or in the mixture. These findings suggest that under the applied potentials, the dibenzothiophene compounds were selectively oxidized by direct and indirect pathways to their corresponding sulfoxides and sulfones without breaking or

mineralizing the aromatic sulfur compounds. The oxidation pathways can then be described as proposed in Fig. 9 and 10.

During the electrolysis of a DBT + 4-MDBT + 4,6-DMBDT mixture in the presence of water at 2.0 V, an excess of ROS is formed. According to the results of the analysis for the electrolyzed solutions by GC-MS and UHPLC-ESI-Q-TOF-MS, these compounds did not compete between them to react with generated ROS. At  $E_{\text{an}} = 1.50$  V, the ratio of these species relative to the substrate in the mixture was low, and only partial conversion was achieved, as described in Fig. 10.

One of the ROS formed during the discharge of water is  $\text{H}_2\text{O}_2$  and then, this oxidizing compound is expected to contribute to the indirect oxidation reaction of the aromatic sulfur compounds. At  $E_{\text{an}} > 1.75$  V, the dibenzothiophene compounds were directly oxidized on the BDD electrode. Simultaneously,  $\text{H}_2\text{O}_2$  was generated *in situ* from reactions (1) and (2) and reacted with the sulfur compounds according to the mechanism proposed in Fig. 11, as also reported previously [42].

### 3.6. Mechanism underlying the direct anodic oxidation of dibenzothiophene compounds on the BDD electrode

Previous publications have pointed out that the oxidation of organic sulfur compounds depends on the water content in acetonitrile [33,36]. Fig. 12 shows a mechanism proposed for the direct anodic oxidation of dibenzothiophenes. It is initiated by an electrochemical step in which an electron is taken from the sulfur atom to yield the reacting cation residue  $[\text{DBT}]^{+\bullet}$ . This cation rapidly undergoes proton loss to yield sulfoxide and other intermediates, followed by a second electron loss to form the sulfone.

### 3.7. BDD electrode stability

The BDD electrode tends to undergo fouling and it is susceptible to delamination or corrosion in the presence of organic compounds at high potentials [43]. The BDD film

surface can also undergo morphological changes. In this context, the BDD anode surface was analyzed by scanning electron microscopy (SEM) after prolonged electrolysis times of 16 h at 2.00 and 3.00 V and after prolonged repetitive cycling of 14 h over a potential interval of  $-0.50$  to  $2.00$  V at  $10 \text{ mV s}^{-1}$ , in the absence and in the presence of 4,6-DMDBT. This analysis was carried out with a JEOL JSM-7800F and revealed that the BDD surface did not undergo neither fouling nor evident morphological changes, as exemplified in SM Fig. S10. The possibility of anodic dissolution of the niobium support in acetonitrile–water after the above assays was also analyzed using ICP-MS. A niobium concentration exceeding 5 ppb was detected. Since this metal is anodically resistive, the detected niobium ions with  $m/z$  93 must have been produced by electrochemical corrosion of the NbC layer formed during the deposition of the BDD film [44].

#### 4. Conclusions

The selective electrochemical oxidation of DBT, 4-MDBT and 4,6-DMDBT to their corresponding sulfoxides or sulfones on BDD anode depended on the applied potential during bulk electrolysis, the water content in the reaction medium and the concentrations of the sulfur compounds. The electrochemical oxidation of a mixture of sulfur compounds containing DBT + 4-MDBT + 4,6-DMDBT revealed that, in acetonitrile (87.5%) –water (12.5%, 0.01 M  $\text{NaNO}_3$ ), the reactivity decreased in the order  $4,6\text{-DMDBT} \geq 4\text{-MDBT} > \text{DBT}$ . The electrochemical oxidation of these compounds occurred at  $E_{\text{an}} \geq 1.75$  V, simultaneously by direct electron transfer at the BDD surface and through ROS that were generated during the electrolysis of water present in the reaction medium. This anodic process was characterized using electrochemical techniques and the corresponding sulfoxides or sulfones were detected by several analytical techniques. Oxidation routes are proposed to explain the formation of such products from each dibenzothiophene compound.

## Acknowledgments

This work was funded by the Benemérita Universidad Autónoma de Puebla (VIEP-BUAP) and by SEP-DGESU. O. Ornelas is grateful for the postdoctoral grant (PRODEP) No. DSA/103.5/16/14302. Support from R. Silva (IFUAP) for SEM analysis is also acknowledged.

## References

- [1] C. Song, An overview of new approaches to deep desulfurization for ultra-clean gasoline, diesel fuel and jet fuel, *Catal. Today* 86 (2003) 211-263.
- [2] S.K. Bej, S.K. Maity, U.T. Turaga, Search for an efficient 4,6-DMDBT hydrodesulfurization catalyst. A review of recent studies, *Energy Fuels* 18 (2004) 1227-1237.
- [3] J.L. García-Gutiérrez, I.P. Lozano, F. Hernández-Pérez, G.C. Laredo, F. Jimenez-Cruz, R & D in oxidative desulfurization of fuels technologies: from chemistry to patents, *Recent Pat. Chem. Eng.* 5 (2012) 174-196.
- [4] F.S. Mjalli, O.U. Ahmed, T. Al-Wahaibi, Y. Al-Wahaibi, I.M. Al Nashef, Deep oxidative desulfurization of liquid fuels, *Rev. Chem. Eng.* 30 (2014) 337-378.
- [5] S.-Y. Dou, R. Wang, Recent advances in new catalysts for fuel oil desulfurization, *Curr. Org. Chem.* 21 (2017) 1019-1036.
- [6] M.N. Hossain H.C. Park, H.S. Choi, A comprehensive review on catalytic oxidative desulfurization of liquid fuel oil, *Catalysts* 9 (2019) 229 (12 pages).
- [7] D. Zheng, W. Zhu, S. Xun, M. Zhou, M. Zhang, W. Jiang, Y. Qin, H. Li, Deep oxidative desulfurization of dibenzothiophene using low-temperature-mediated titanium dioxide catalyst in ionic liquids, *Fuel* 159 (2015) 446-453.

- [8] Y. Li, Y. Zhang, P. Wu, C. Feng, G. Xue, Catalytic oxidative/extractive desulfurization of model oil using transition metal substituted phosphomolybdates-based ionic liquids, *Catalysts* 8 (2018) 639 (13 pages).
- [9] A. Haghghat Mamaghani, S. Fatemi, M. Asgari, Investigation of influential parameters in deep oxidative desulfurization of dibenzothiophene with hydrogen peroxide and formic acid, *Int. J. Chem. Eng.* 2013 (2013) 1-10.
- [10] M. Te, C. Fairbridge, Z. Ring, Oxidation reactivities of dibenzothiophenes in polyoxometalate/H<sub>2</sub>O<sub>2</sub> and formic acid/H<sub>2</sub>O<sub>2</sub> systems, *Appl. Catal. A: Gen.* 219 (2001) 267-280.
- [11] F. Al-Shahrani, T. Xiao, S.A. Llewellyn, S. Barri, Z. Jiang, H. Shi, G. Martinie, M.L.H. Green, Desulfurization of diesel via the H<sub>2</sub>O<sub>2</sub> oxidation of aromatic sulfides to sulfones using a tungstate catalyst, *Appl. Catal. B: Environ.* 73 (2007) 311-316.
- [12] P.A. Michaud, M. Panizza, L. Ouattara, T. Diaco, G. Foti, Ch. Comninellis, Electrochemical oxidation of water on synthetic boron-doped diamond thin film anodes, *J. Appl. Electrochem.* 33 (2003) 151-154.
- [13] I. Kisacik, A. Stefanova, S. Ernst, H. Baltruschat, Oxidation of carbon monoxide, hydrogen peroxide and water at a boron doped diamond electrode: the competition for hydroxyl radicals, *Phys. Chem. Chem. Phys.* 15 (2013) 4616-4624.
- [14] B. Marselli, J. García-Gomez, P.A. Michaud, M.A. Rodrigo, Ch. Comninellis, Electrogeneration of hydroxyl radicals on boron-doped diamond electrodes, *J. Electrochem. Soc.* 150 (2003) D79-D83.
- [15] V. Lam, G. Li, Ch. Song, J. Chen, C. Fairbridge, A review of electrochemical desulfurization technologies for fossil fuels, *Fuel Process. Technol.* 98 (2012) 30-38.

- [16] W. Wang, S. Wang, Y. Wang, H. Liu, Z. Wang, A new approach to deep desulfurization of gasoline by electrochemically catalytic oxidation and extraction, *Fuel Process. Technol.* 88 (2007) 1002-1008.
- [17] W. Wang, S. Wang, H. Liu, Z. Wang, Desulfurization of gasoline by a new method of electrochemical catalytic oxidation, *Fuel* 86 (2007) 2747-2753.
- [18] X.D. Tang, T. Hu, J.J. Li, F. Wang, D.Y. Qing, Deep desulfurization of condensate gasoline by electrochemical oxidation and solvent extraction, *RSC Adv.* 5 (2015) 53455-53461.
- [19] Z. Alipoor, A. Behrouzifar, S. Rowshanzamir, M. Bazmi, Electrooxidative desulfurization of a thiophene-containing model fuel using a square wave potentiometry technique, *Energy Fuels* 29 (2015) 3292-3301.
- [20] X. Du, Y. Yang, C. Yi, Y. Chen, C. Cai, Z. Zhang, Preparation of AAO-CeO<sub>2</sub> nanotubes and their application in electrochemical oxidation desulfurization of diesel, *Nanotechnology* 28 (2017) 065708.
- [21] D. Julião, A.C. Gomes, M. Pillinger, R. Valença, J.C. Ribeiro, I.S. Gonçalves, S.S. Balula, Desulfurization of liquid fuels by extraction and sulfoxidation using H<sub>2</sub>O<sub>2</sub> and [CpMo(CO)<sub>3</sub>R] as catalysts, *Appl. Catal. B: Environ.* 230 (2018) 177-183.
- [22] D. Liu, M. Li, R.L. Al-Otaibi, L. Song, W. Li, Q. Li, H.O. Almigrin, Z. Yan, Study on the desulfurization of high-sulfur crude oil by the electrochemical method, *Energy Fuels* 29 (2015) 6928-6934.
- [23] X.D. Tang, T. Hu, J.J. Li, F. Wang, D.Y. Qing, Desulfurization of kerosene by the electrochemical oxidation and extraction process, *Energy Fuels* 29 (2015) 2097-2103.
- [24] C. Shu, T. Sun, J. Jia, Z. Lou, A novel desulfurization process of gasoline via sodium metaborate electroreduction with pulse voltage using a boron-doped diamond thin film electrode, *Fuel* 113 (2013) 187-195.

- [25] M. Panizza, G. Cerisola, Influence of anode material on the electrochemical oxidation of 2-naphthol. Part 1. Cyclic voltammetry and potential step experiments, *Electrochim. Acta* 48 (2003) 3491-3497.
- [26] A. Jailson-Cabral da Silva, E. Vieira dos Santos, C.C. de Oliveira-Morais, C.A. Martínez-Huitle, S. Souza Leal Castro, Electrochemical treatment of fresh, brine and saline produced water generated by petrochemical industry using Ti/IrO<sub>2</sub>-Ta<sub>2</sub>O<sub>5</sub> and BDD in flow reactor, *Chem. Eng. J.* 233 (2013) 47-55.
- [27] A.R.F. Pipi, I. Sirés, A.R. De Andrade, E. Brillas, Application of electrochemical advanced oxidation processes to the mineralization of the herbicide diuron, *Chemosphere* 109 (2014) 49-55.
- [28] S. Lanzalaco, I. Sirés, A. Galia, M.A. Sabatino, C. Dispenza, O. Scialdone, Facile crosslinking of poly(vinylpyrrolidone) by electro-oxidation with IrO<sub>2</sub>-based anode under potentiostatic conditions, *J. Appl. Electrochem.* 48 (2018) 1343-1352.
- [29] I. Sirés, E. Brillas, M.A. Oturan, M.A. Rodrigo, M. Panizza, Electrochemical advanced oxidation processes: Today and tomorrow. A review, *Environ. Sci. Pollut. Res.* 21 (2014) 8336-8367.
- [30] M. Panizza, E. Brillas, Ch. Comninellis, Application of boron-doped diamond electrodes for wastewater treatment, *J. Environ. Eng. Manage.* 18 (2008) 139-153.
- [31] H. Zanin, R.F. Teófilo, A.C. Peterlevitz, U. Oliveira, J.C. de Paiva, H.J. Ceragioli, E.L. Reis, V. Baranauskas, Diamond cylindrical anodes for electrochemical treatment of persistent compounds in aqueous solution, *J. Appl. Electrochem.* 43 (2013) 323-330.
- [32] S. Mitroka, S. Zimmeck, D. Troya, J.M. Tanko, How solvent modulates hydroxyl radical reactivity in hydrogen atom abstractions, *J. Am. Chem. Soc.* 132 (2010) 2907-2913.



- [33] E. Méndez-Albores, M. González-Fuentes, M.M. Dávila-Jiménez, F.J. González, Role of water in the formation of sulfoxide and sulfone derivatives during the electrochemical oxidation of dibenzothiophene in acetonitrile, *J. Electroanal. Chem.* 751 (2015) 7-14.
- [34] G. Bontempelli, F. Magno, G.A. Mazzocchin, Cyclic and A.C. voltammetric study of dibenzothiophene in acetonitrile medium, *J. Electroanal. Chem. Interfacial Electrochem.* 43 (1973) 377-385.
- [35] D.S. Houghton, A.A. Humffray, Anodic oxidation of diaryl sulphides-I. Diphenyl sulphide in sulphate and perchlorate media, *Electrochim. Acta* 17 (1972) 1421-1433.
- [36] P.T. Cottrell, C.K. Mann, Electrochemical oxidation of aliphatic sulfides under nonaqueous conditions, *J. Electrochem. Soc.* 116 (1969) 1499-1503.
- [37] J.L. Rivera, P. Navarro-Santos, L. Hernández-González, R. Guerra-González, Reactivity of alkyldibenzothiophenes using theoretical descriptors, *J. Chem.* 2014 (2014) 1-8.
- [38] Y. He, W. Huang, R. Chen, W. Zhang, H. Lin, Improved electrochemical performance of boron-doped diamond electrode depending on the structure of titanium substrate, *J. Electroanal. Chem.* 758 (2015) 170-177.
- [39] J.N. Soderberg, A.C. Co, A.H.C. Sirk, V.I. Birss, Impact of porous electrode properties on the electrochemical transfer coefficient, *J. Phys. Chem. B* 110 (2006) 10401-10410.
- [40] J. Iniesta, P.A. Michaud, M. Panizza, G. Cerisola, A. Aldaz, Ch. Comminellis, Electrochemical oxidation of phenol at boron-doped diamond electrode, *Electrochim. Acta* 46 (2001) 3573-3578.
- [41] J.F. Zhi, H.B. Wang, T. Nakashima, T.N. Rao, A. Fujishima, Electrochemical incineration of organic pollutants on boron-doped diamond electrode. Evidence for direct electrochemical oxidation pathway, *J. Phys. Chem. B* 107 (2003) 13389-13395.

- [42] E.N. Al-Shafei, Process for in-situ electrochemical oxidative generation and conversion of organosulfur compounds, U.S. Patent, No. US 2013/0053578 A1, 2013.
- [43] T. Kashiwada, T. Watanabe, Y. Ootani, Y. Tateyama, Y. Einaga, A study on electrolytic of boron-doped diamond electrodes when decomposing organic compounds, ACS Appl. Mater. Interfaces 8 (2016) 28299-28305.
- [44] G.A. Orjuela, R. Rincón, J.J. Olaya, Corrosion resistance of niobium carbide coatings produced on AISI 1045 steel via thermo-reactive diffusion deposition, Surf. Coat. Tech. 259 (2014) 667-675.

ACCEPTED MANUSCRIPT

**Figure captions**

**Fig. 1.** Chemical structure of dibenzothiophene (DBT), 4-methyldibenzothiophene (4-MDBT), and 4,6-dimethyldibenzothiophene (4,6-DMDBT).

**Fig. 2.** Linear sweep voltammograms obtained on a 20 cm<sup>2</sup> BDD electrode immersed in 80 mL of 67 mg L<sup>-1</sup> DBT in different electrolytes: (a) Acetonitrile (87.5%)-water (12.5%, 0.01 M NaNO<sub>3</sub>), (b) acetonitrile (12.5%)-water (87.5%, 0.01 M NaNO<sub>3</sub>) and (c) water (100%, 0.01 M NaNO<sub>3</sub>). Scan rate 10 mV s<sup>-1</sup>.

**Fig. 3.** a, linear polarization curves on a BDD electrode recorded in acetonitrile (87.5%)-water (12.5%, 0.01 M NaNO<sub>3</sub>), (-----) in the absence of dibenzothiophene or in the presence of (a) 67 mg L<sup>-1</sup> DBT, (b) 86 mg L<sup>-1</sup> 4-MDBT and (c) 86 mg L<sup>-1</sup> 4,6-DMDBT. b, after subtracting the background current from the (a') 67 mg L<sup>-1</sup> DBT curve, (b') 86 mg L<sup>-1</sup> 4-MDBT curve and (c') 86 mg L<sup>-1</sup> 4,6-DMDBT. Scan rate 10 mV s<sup>-1</sup>.

**Fig. 4.** a, consecutive cyclic voltammograms (cycles 1–5) on a BDD anode in acetonitrile (87.5%)-water (12.5%, 0.01 M NaNO<sub>3</sub>), (-----) in the absence of dibenzothiophene or in the presence of (a) 67 mg L<sup>-1</sup> DBT, (b) 86 mg L<sup>-1</sup> 4-MDBT and (c) 86 mg L<sup>-1</sup> 4,6-DMDBT. b, (a) consecutive cycles (1–5) for 200 mg L<sup>-1</sup> DBT and (b) consecutive cycles (1-44) for 200 mg L<sup>-1</sup> 4,6-DMDBT under the same conditions. Scan rate 10 mV s<sup>-1</sup>.

**Fig. 5.** Cyclic voltammograms recorded using a BDD anode in acetonitrile (87.5%)-water (12.5%, 0.01 M NaNO<sub>3</sub>). (-----) in the absence of dibenzothiophene. In a, (a) 30 mg L<sup>-1</sup>, (b) 67 mg L<sup>-1</sup> and (c) 100 mg L<sup>-1</sup> of DBT. In b, (a') 30 mg L<sup>-1</sup> (b') 100 mg L<sup>-1</sup> and (c') 150 mg L<sup>-1</sup> of 4,6-DMDBT. The inset panels show the corresponding Tafel analysis. Scan rate 10 mV s<sup>-1</sup>.

**Fig. 6.** Linear sweep voltammograms obtained after subtracting the background current in acetonitrile (87.5%)-water (12.5%, 0.01 M NaNO<sub>3</sub>). In a, (a) 30 mg L<sup>-1</sup>, (b), 67 mg L<sup>-1</sup> and (c) 100 mg L<sup>-1</sup> of DBT. In b, (a') 30 mg L<sup>-1</sup>, (b'), 100 mg L<sup>-1</sup> and (c') 150 mg L<sup>-1</sup> of 4,6-DMDBT. The upper insets show *I* vs. concentration at 1774 mV in fig. a or 1884 mV in fig. b. The lower insets show *E* vs. concentration at 0.525 (curve 1) or 0.750 mA (curve 2) in fig. and b, respectively. Scan rate 10 mV s<sup>-1</sup>.

**Fig. 7.** Potentiostatic *I*-*t* curves in quiescent solutions recorded (---) in the absence of dibenzothiophene or in the presence of different 4,6-DMDBT concentrations: In a, (a) 30 mg L<sup>-1</sup>, (b) 86 mg L<sup>-1</sup> and (c) 200 mg L<sup>-1</sup> at *E*<sub>an</sub> = 1.15 V; in b, (a) 30 mg L<sup>-1</sup>, (b) 100 mg L<sup>-1</sup> and (c) 150 mg L<sup>-1</sup> at *E*<sub>an</sub> = 1.50 V; and in c, (a) 30 mg L<sup>-1</sup>, (b) 86 mg L<sup>-1</sup>, (c) 100 mg L<sup>-1</sup> and (d) 200 mg L<sup>-1</sup> at *E*<sub>an</sub> = 2.00 V. In the insets, the slope of the linear correlations was: a, 0.217 μA mg L<sup>-1</sup>; b, 2.89 μA mg L<sup>-1</sup>; and c, 5.84 μA mg L<sup>-1</sup>.

**Fig. 8.** Chronoamperometric response of the BDD anode during the step-by-step injection of a, water or b, 4,6-DMDBT into the reaction system. The anodic potential was 1.75 V. The arrows indicate the injection into the reaction system of water (⊙) or 4,6-DMDBT (↓). The insets show *I* vs. the corresponding concentration.

**Fig. 9.** Scheme for the electrochemical oxidation of 4,6-DMDBT to yield the corresponding sulfoxide and sulfone at 1.50 and 2.00 V in acetonitrile (87.5%)-water (12.5%, 0.01 M NaNO<sub>3</sub>).

**Fig. 10.** Scheme for the electrochemical oxidation of a mixture of DBT + 4-MDBT + 4,6-DMDBT to yield their corresponding sulfoxides and sulfones at 1.50 and 2.00 V in acetonitrile (87.5%)-water (12.5%, 0.01 M NaNO<sub>3</sub>).

**Fig. 11.** Oxidation reactions of the dibenzothiophene compounds with hydrogen peroxide generated *in situ* by water electrolysis.

**Fig. 12.** Scheme of the direct electrochemical oxidation of dibenzothiophene compounds on a BDD anode in acetonitrile (87.5%)-water (12.5%, 0.01 M NaNO<sub>3</sub>).

ACCEPTED MANUSCRIPT

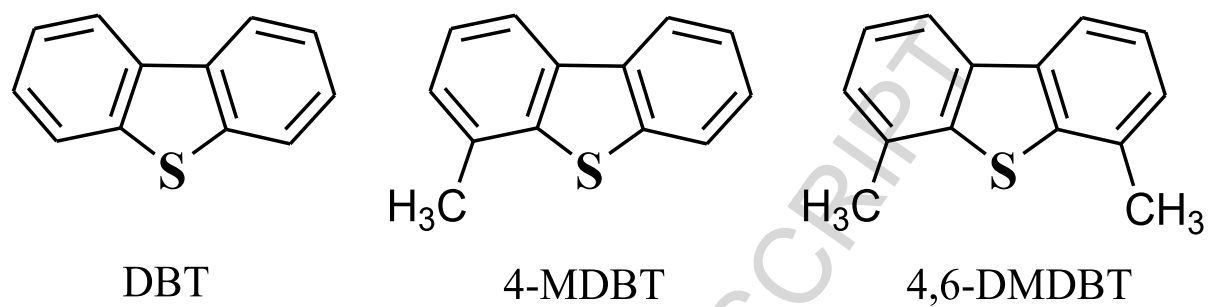


Fig. 1

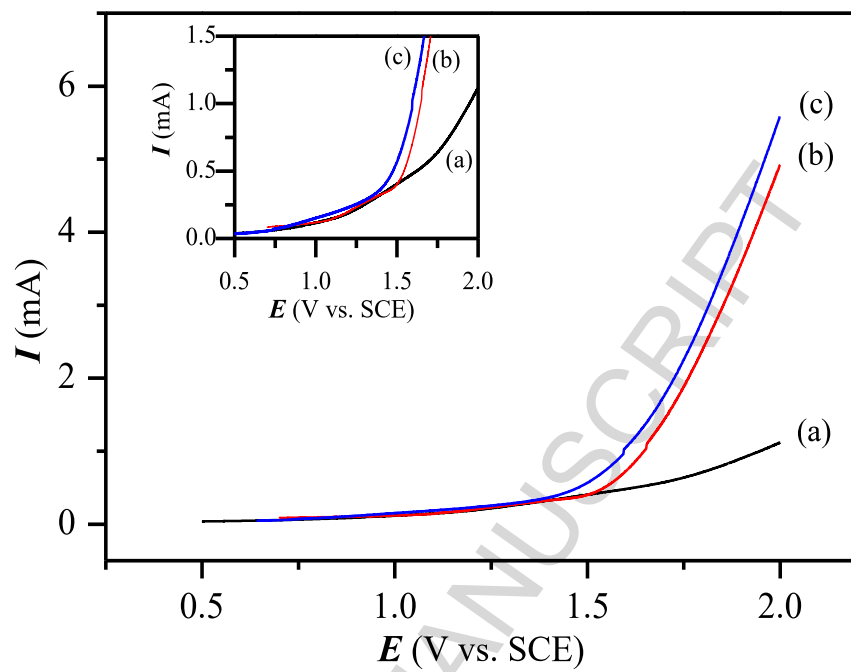


Fig. 2

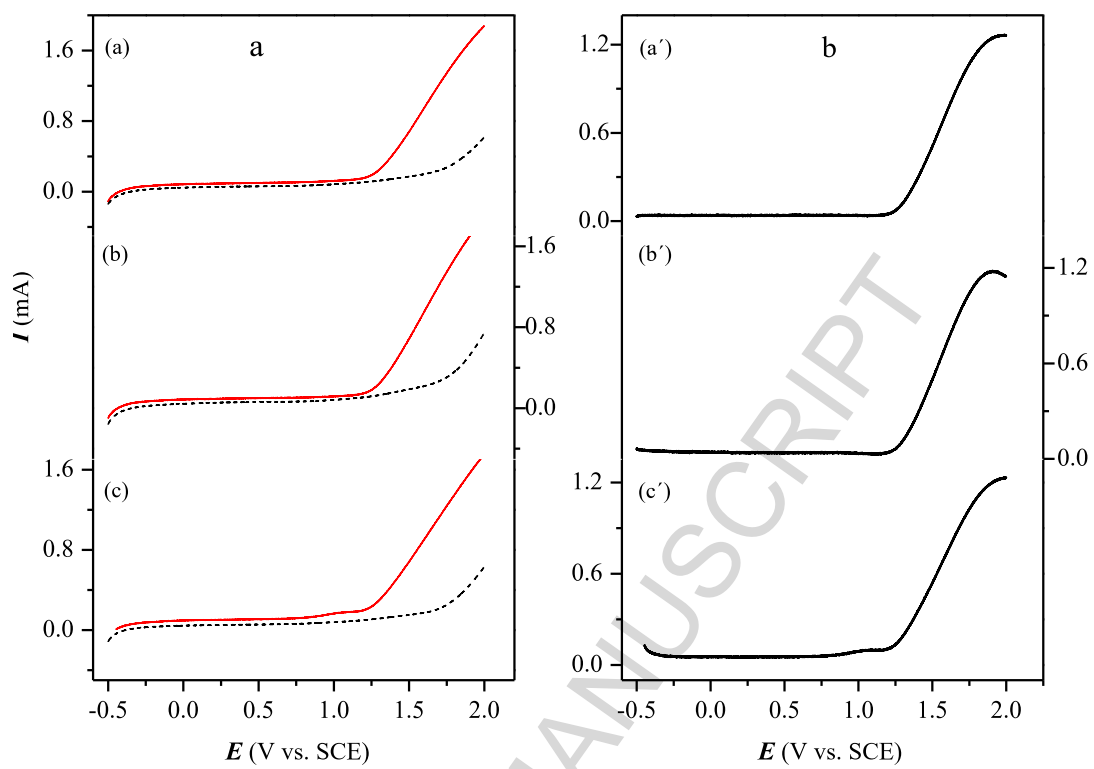


Fig. 3



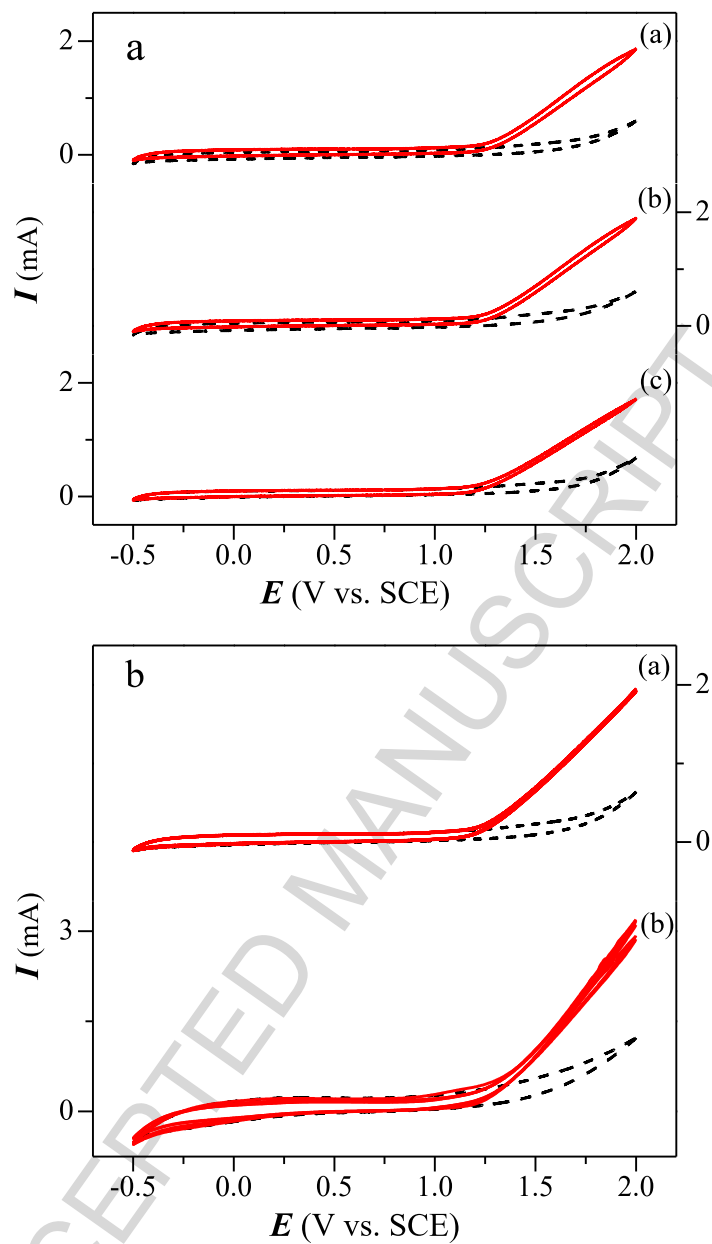


Fig. 4

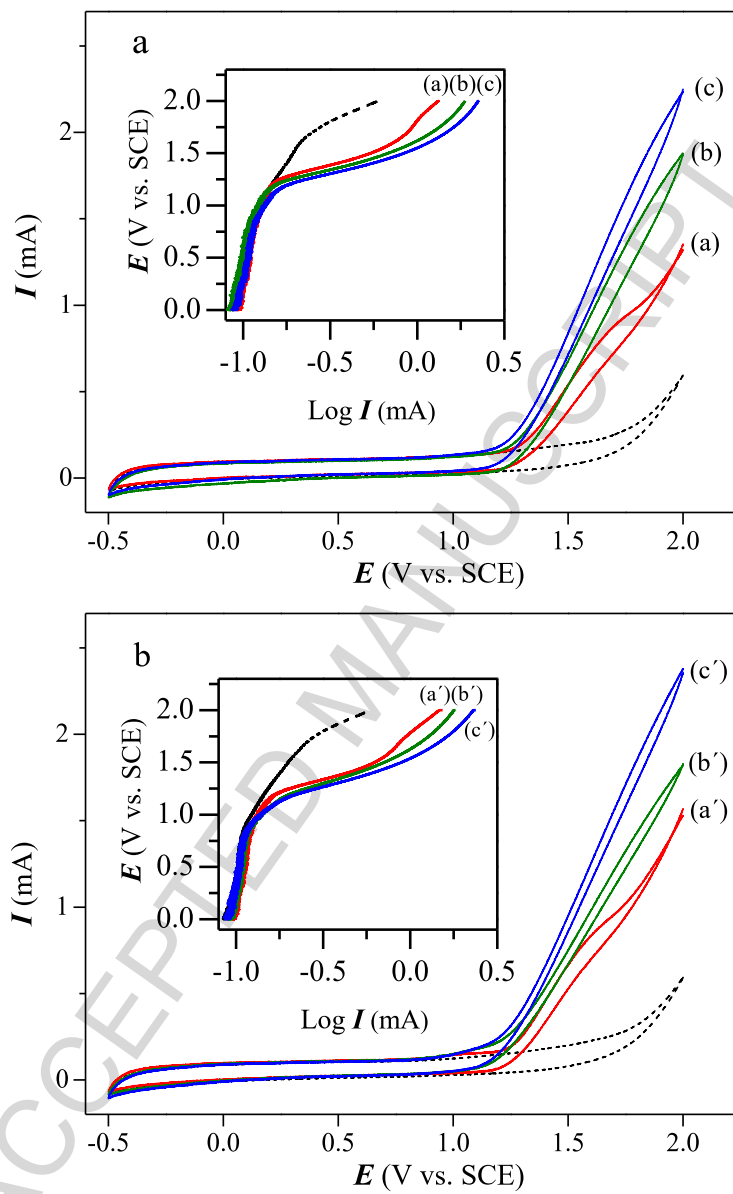


Fig. 5

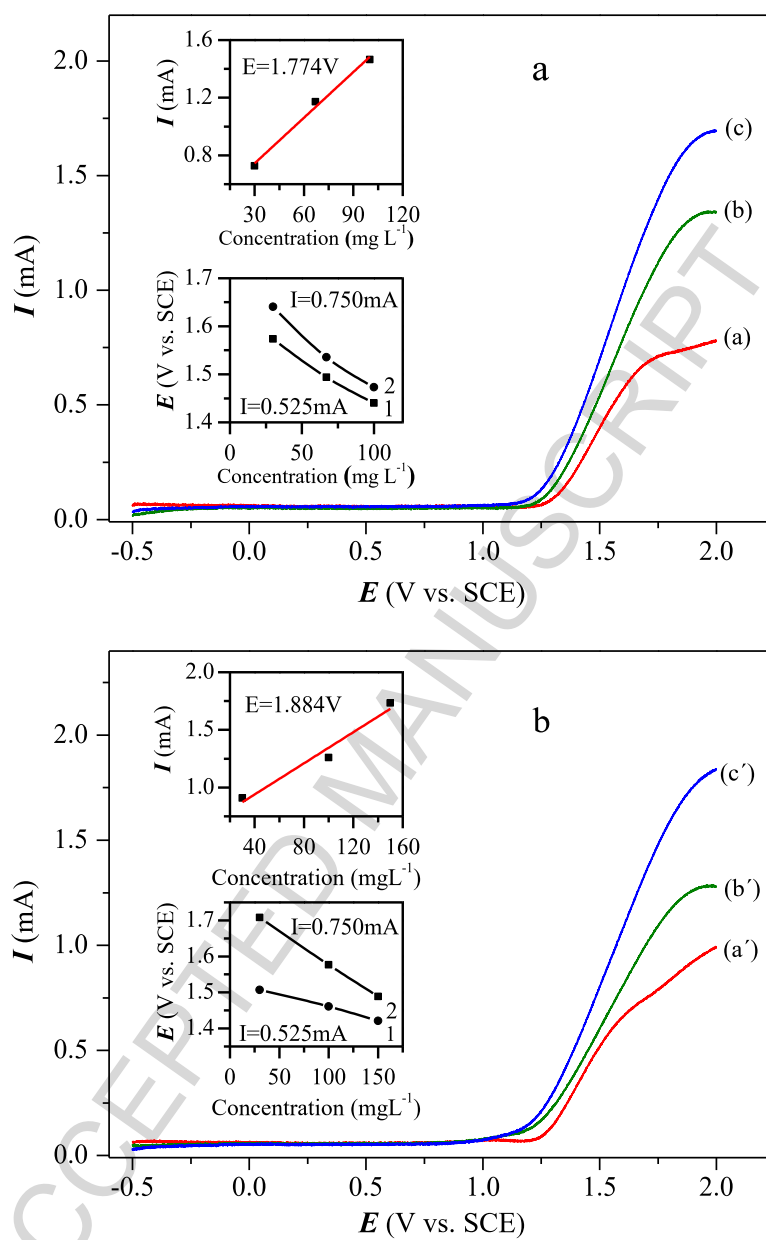


Fig. 6

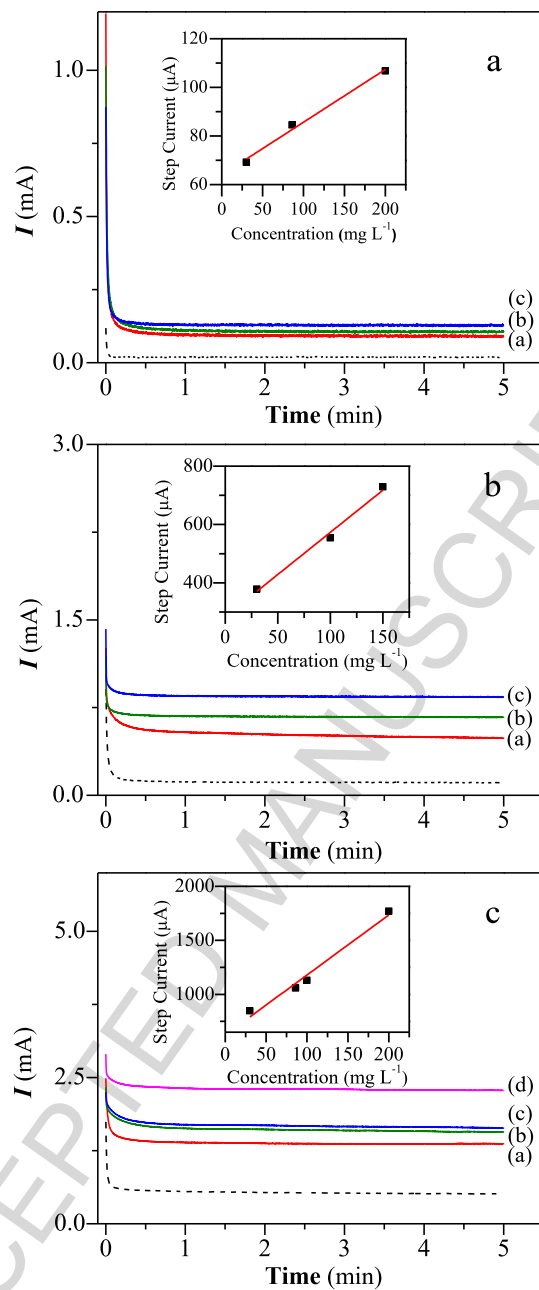


Fig. 7

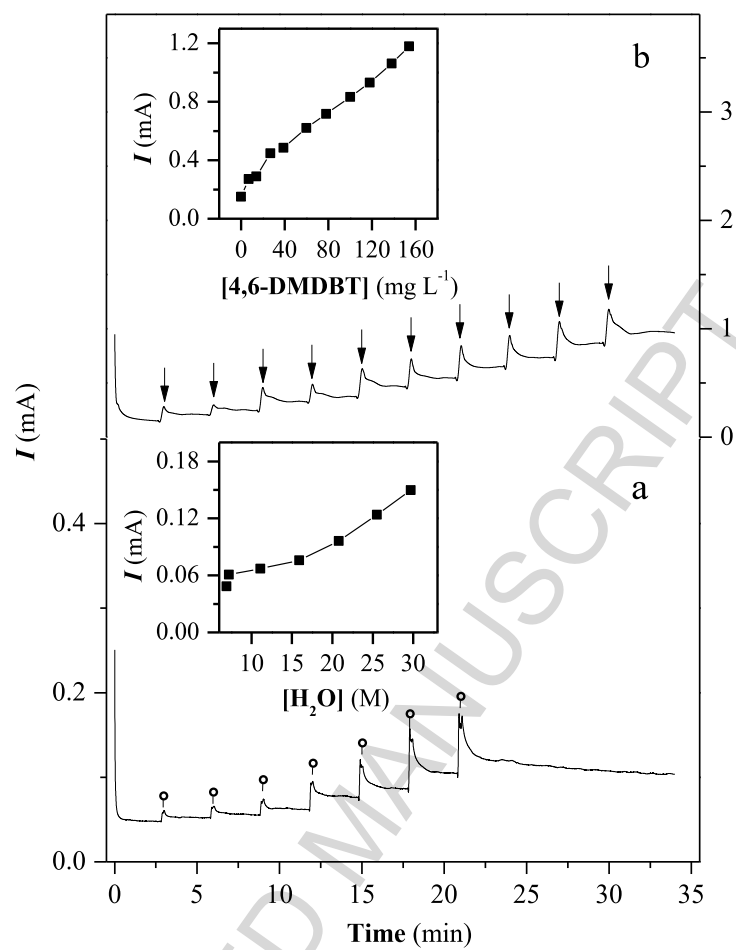


Fig. 8

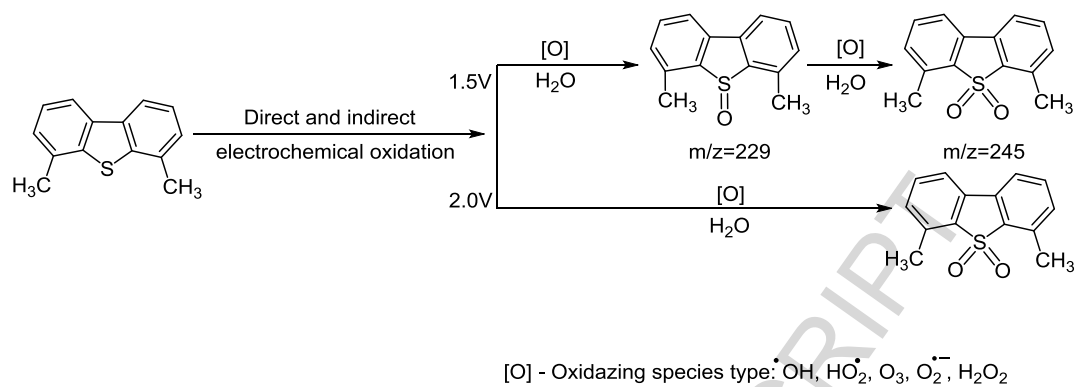


Fig. 9

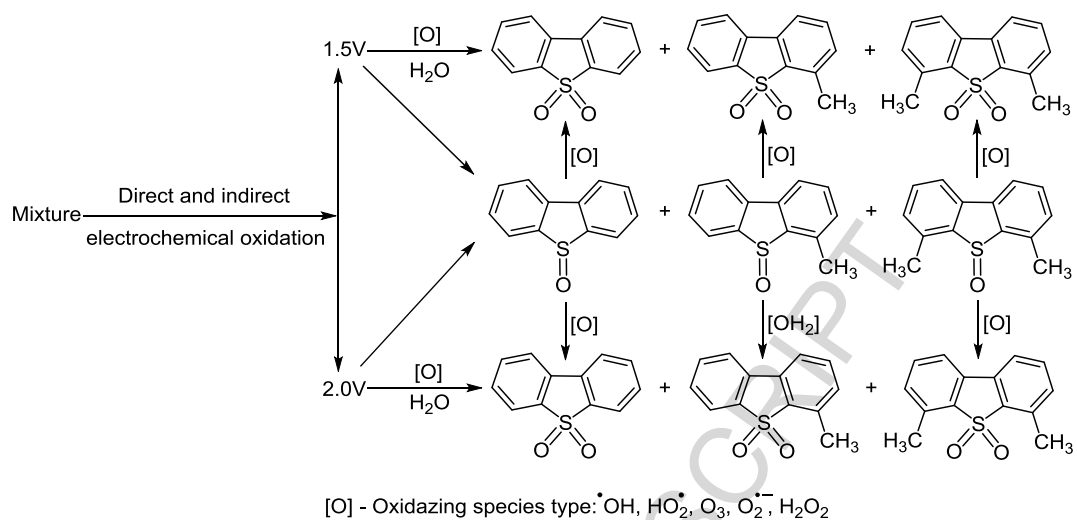


Fig. 10

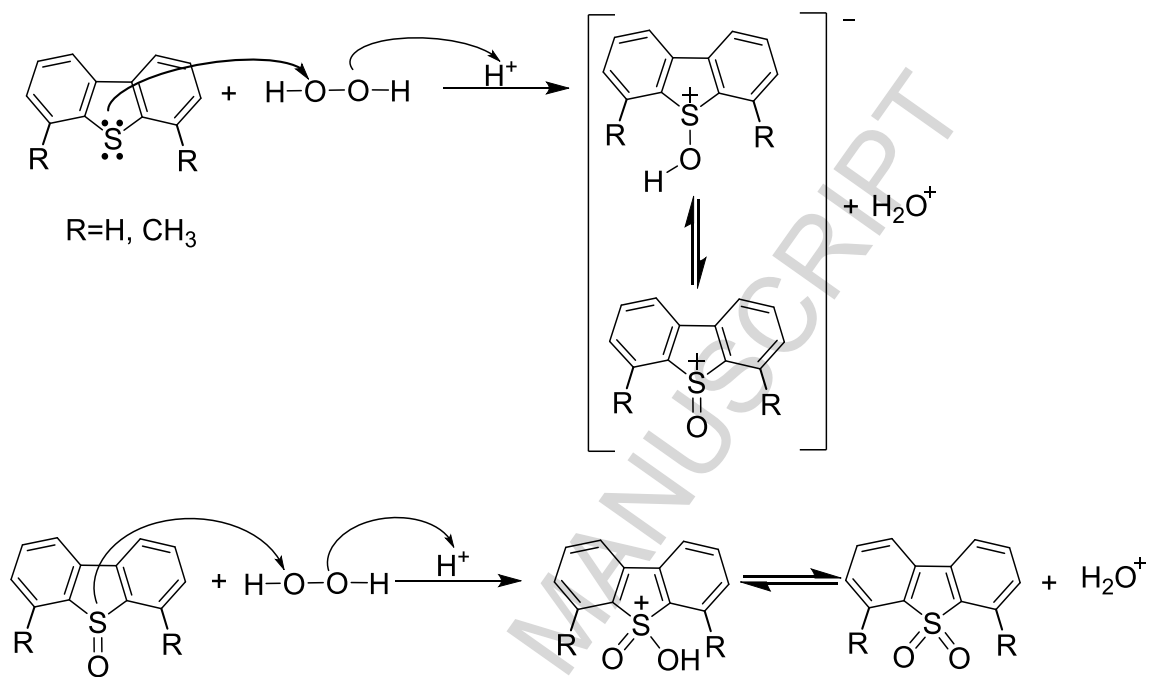


Fig. 11



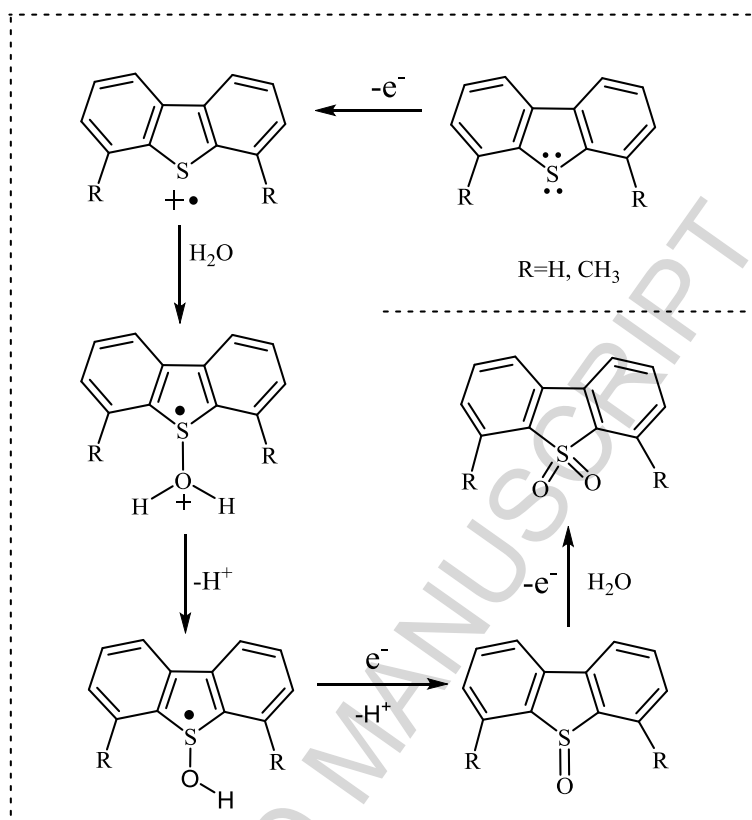
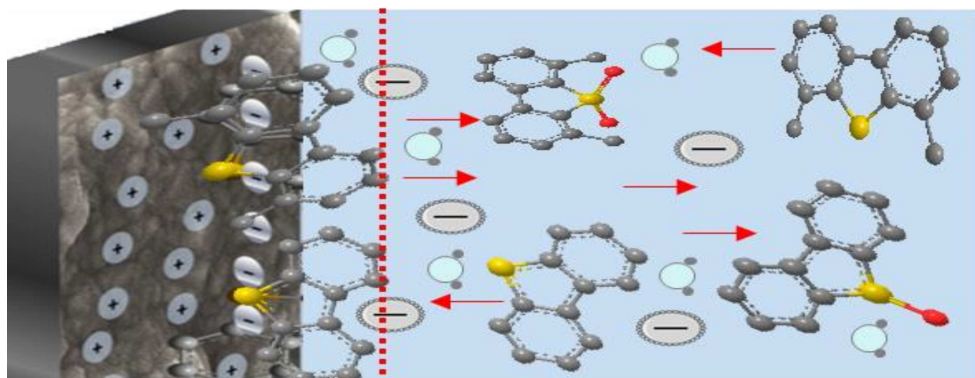


Fig. 12

## Graphical abstract



ACCEPTED MANUSCRIPT

**RESEARCH HIGHLIGHTS**

- Electrochemical oxidation of dibenzothiophenes in CH<sub>3</sub>CN/H<sub>2</sub>O using a BDD anode
- Oxidation is direct or mediated by reactive oxygen species like •OH
- Selective oxidation of single compounds or mixtures to sulfoxides or sulfones
- The conversion depends on concentration, applied potential and water content
- The electrochemical reactivity on BDD decreases as: 4,6-DMDBT ≥ 4-MDBT > DBT